Automated Segmentation of Cerebral Ventricular Compartments

Y. Wu[1], K. M. Pohl[2], S. K. Warfield[3], C. R. Guttmann[1]

[1]Center for Neurological Imaging, Brigham & Women's Hospital, Boston, MA, United States, [2]Artificial Intelligence Laboratory, Massachusetts Institute of Technology, Boston, MA, United States, [3]Surgical Planning Laboratory, Brigham & Women's Hospital, Boston, MA, United States

Synopsis: Fully automated segmentation of cerebral ventricle chambers, which is designed to discriminate the lateral, third and fourth ventricles, as well as the aqueduct is presented and validated. A novel topology-restricted intensity-based algorithm was extended by incorporating a ventricle probability model for ventricle segmentation, and validated on 124 coronal SPGR sections of a healthy volunteer's brain. 3D-rendering of the segmented ventricles showed good qualitative delineation of ventricular compartments. Comparison with a radiologist's manual delineation showed excellent agreement. We expect this method to be useful in clinical studies involving ventricular morphometry and for improving the segmentation of white matter lesions.

Introduction: The segmentation of ventricles is important for accurate segmentation of white matter lesions, e.g. in MS. by reducing the misclassification of lesions caused by choroid plexus and partial volume artifacts at the surface of ventricles. Also, one in five hundred newborn in U.S. suffers from congenital or acquired hydrocephalus. Hydrocephalus also occurs in adults as a result of head trauma, meningitis, tumors or cysts. Enlarged ventricles are also observed in AD, MS and schizophrenia patients. The quantitative measurement, as well as 3D display of ventricles using segmentation *in vivo* can be expected to be of value in differential diagnosis, disease characterization and follow-up. Manual segmentation of ventricles is tedious and requires good neuroanatomical knowledge. Specific neuroanatomic knowledge is required especially when outlining structures where partial volume artifacts limit the conspicuity of CSF-filled structures: the third ventricle, the boundary between optic recess and infundibulum recess (tuber cinereum) to the chiasmatic cistern and interpeduncular cistern, and also the boundary between the pineal gland recess and the great cerebral vein cistern. Several semi-automated or automated approaches of ventricle segmentation proposed, none of them distinguishes between lateral ventricles, the third, the fourth, and the aqueduct (1). In this study, the novel segmentation Expectation Maximization-Field Approximation-Local Prior algorithm (EM-MF-LP) (2) that combines intensity-based statistical segmentation and topologic constraints was implemented to segment all the compartments of ventricular system.

Methods: EM-MF-LP uses a brain prior probability map (PPM) that was derived from 82 different brains (3). Previously, anatomical information of the ventricle system was **not** included in this PPM. Therefore, ventricular compartment labels were added to derive a new PPM applicable to ventricle segmentation. These ventricular compartment labels (left and right lateral, third and fourth ventricle and aqueduct) were delineated by a radiologist with expert knowledge of ventricular substructures. The left and right lateral ventricles were labeled individually. The separation between the two lateral ventricles was drawn at the approximate location of the Septum. Each lateral ventricle consists of frontal horn, occipital horn, temporal horn, which are connected to lateral ventricle trigone and body. The third ventricle was defined as below the interventricular foramina. The fourth ventricle and the cerebral aqueduct were also outlined. The new PPM containing ventricular compartments was then combined with the PPM of the remaining brain structures. 124 coronal slices of SPGR T1-weighted MRI of a normal volunteer brain were used to test the method (voxel size of 0.9375x0.9375x1.5 mm). Using a state of the art non-rigid registration algorithm (4), the new brain PPM with ventricle location priors, was deformed to match the subject brain. The EM-MF algorithm then iterates between bias field estimation and tissue segmentation under spatial information constraints to acquire the segmentation of ventricles, as well as other brain structures. A qualitative assessment of the automated segmentation was obtained by a 3D surface rendering (Figure d) of the segmented ventricle (directly without any human editing). To quantitatively assess the performance of this method, a radiologist manually segmented 16 slices of two lateral and third ventricles, four slices of fourth ventricle, and two slices of the aqueduct. DSC (5) was used to evaluate the accuracy against the radiologist's hand drawing (Figure e).

Results: Lateral ventricles were accurately segmented and separated into two parts with details of frontal, occipital, and temporal horns. The third ventricle shows details of optic recess, infundibular recess and the pineal gland recess, as well as the interthalamic adhesion. The aqueduct and the fourth ventricle were also successfully segmented (Figure a through c).

The average DSC comparing automated to radiologist's manual segmentation of left lateral, right lateral, third and fourth ventricle were 0.801, 0.852, 0.723 and 0.732 respectively. DSC above 0.70 is commonly considered excellent agreement (5). The narrow structure of the aqueduct also achieved DSC of 0.508.

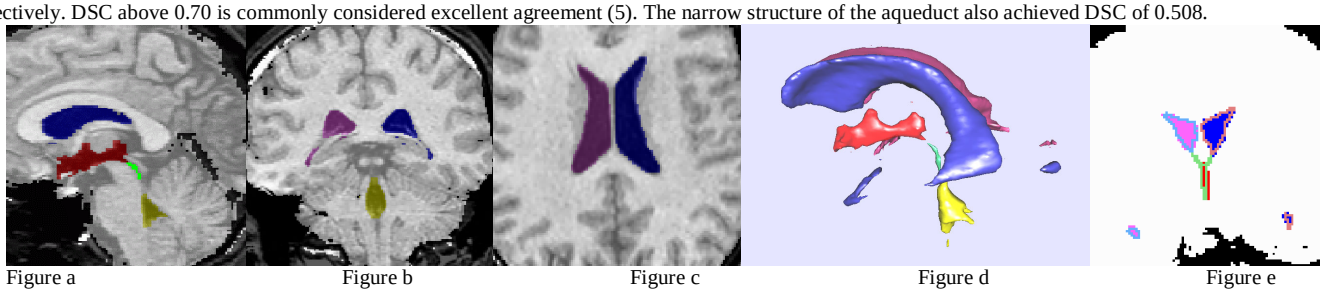

Figure a Figure b Figure c Figure d Figure e

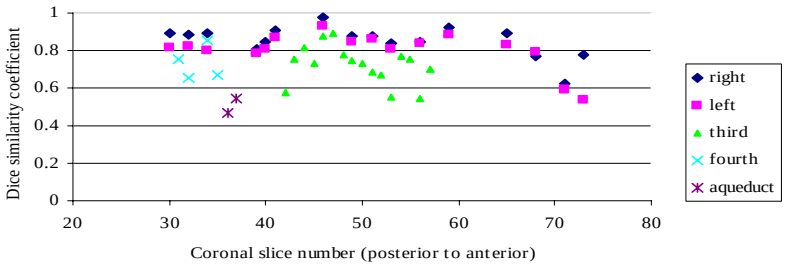

***Figure a to c**: Automated ventricle segmentation results overlaid on three planar reformates of SPGR MRI; this demonstrates accurate delineation of left lateral (purple), right lateral (blue), third (red), fourth (orange) ventricles and aqueduct (green). **Figure d**: A 3D representation of ventricular segmentation using the automated method, without any manual editing. **Figure e**: Automated ventricle segmentation overlaid with the radiologist's manual delineation (cyan, orange, green) of two lateral ventricles, the third ventricle (in the center) and lateral ventricle temporal horns in a coronal plane. **Chart**: DSC results against coronal slice number (posterior to anterior). Note the the consistency of the performance throughout the brain volume.*

Conclusion: Combination of intensity-based segmentation and topological constraints yields excellent qualitative and quantitative segmentation of ventricular brain structures. We expect this method to be useful in clinical studies involving ventricular morphometry and for improving the segmentation of white matter lesions.

Reference:

1. Schnack H.G., et al. Neuroimage, 14:95-104, 2001
2. Pohl M.K. et al., MICCAI'2002 Part I., 564-571
3. Warfield S.K., et al. MICCAI'2001, 266-274
4. Guimond A., IEEE Trans Med Imaging, Vol.20, 58-69, 2001
5. Zijdenbos A.P., et al., IEEE Trans Med Imaging, Vol.13, 716-724, 1999